Int. J. Electrochem. Sci., 14 **(2019)** 4271 – 4279, doi: 10.20964/2019.05.59

International Journal of
ELECTROCHEMICAL
SCIENCE
www.electrochemsci.org

Short Communication

A Sensitive Electrochemical Impedance DNA Biosensor Based on ZnO Nanorod Electrodes for BCR/ABL Fusion Gene Detection

Jiao-yun Xia[*], *Jing Qing*, *Jun-jie Liu*

College of Chemistry and Biological Engineering, Changsha University of Science and Technology, 960, 2nd Section, Wanjiali South RD, Changsha 410114, P. R. China
[*]E-mail: xiajy625@163.com, xiajiaoyun@foxmail.com

Received: 10 January 2019 / *Accepted:* 6 March 2019 / *Published:* 10 April 2019

A ZnO based DNA biosensor was developed to detect complementary target single-stranded DNA (ssDNA) of BCR/ABL fusion gene. ZnO nanorods (NRs) have been synthesized onto platinized silicon (Pt/Si) substrate using facile and economical chemical bath deposition method. The ssDNA probe was immobilized by electrostatic attraction on the ZnO/Pt/Si surface. The morphology of the samples were characterized by scanning electron microscopy. Electrochemical impedance spectroscopy and cyclic voltammetry were done to study ZnO NR arrays, and the immobilization and the hybridization of ssDNA at the electrode surface. The fabricated DNA biosensor was evaluated in the complementary target ssDNA of BCR/ABL probe in the dynamic range from 1.0 pM/L to 1.0 nM/L which indicates a good linearity, high sensitivity and low detection limit of 2.75×10^{-13} mol/L. The successful detection of BCR/ABL fusion gene exhibits its potential to be a robust and sensitive label-free electrochemical impedance measurement for sensing applications.

Keywords: Electrochemical impedance DNA biosensor; BCR/ABL fusion gene; Cyclic voltammetry; Electrochemical impedance spectroscopy

1. INTRODUCTION

Zinc oxide (ZnO) is one of the most promising candidates for the DNA biosensor due to its wonderful biocompatibility, good chemical stability and easy surface modification [1, 2]. It is widely recognized that the solid substrate for immobilizing probe DNA would be nontoxic, biocompatible, and chemically stable. Silicon, carbon, and gold materials were extensively used as solid platforms to examine the target DNA sequences [3-5]. Gene chips and DNA biosensors are of major interest because of their wonderful applications to achieve sequence- specific information in a rapid, cheaper and simpler method Compared to conventional hybridization technique [6]. Nowadays, nucleic acid recognition processes based DNA biosensors are developing for economical, simple and rapid testing of infectious

and genetic diseases [7]. DNA sensors can be prepared by immobilizing single stranded DNA (ssDNA) probes onto various electrodes via electroactive indicators to evaluate the hybridization process [8].

BCR/ABL fusion gene is the traditional gene which exists in almost all chronic myelogenous leukemia patients [9]. Therefore, the BCR/ABL fusion gene detection allows an early diagnosis and control of the disease, which improves the ability to detect at least the remaining leukemia cells, particularly after bone marrow transplant [10].

In recent years, electrochemical DNA biosensor has been well known as a hopeful method for the detection of sequence-specific DNA hybridization because the electrochemical signaling techniques are specific, sensitive, simple and cost-effective [11].

Chen had synthesized 2-nitroacridone as the redox label for DNA hybridization. The fabricated sensor shows linear response to complementary DNA target with a detection limit of 6.7 10^{-9} M [12].

The primary electrochemical DNA studies are focused on the reduction or oxidation of DNA with high molecular weight on a mercury electrode [13]. Millan and Mikkelsen had used small electroactive molecules to separate double-stranded DNA and ssDNA by immobilizing DNA probe on carbon electrodes [14]. Lin had provided an electrochemical DNA biosensor based on Au-nanoparticles/poly-eriochrome electrode for BCR/ABL fusion gene analyze. They introduced a technique for immobilizing hairpin capture probe by nanogold bound. Then, methylene blue accumulated for detection of DNA hybridization [15].

In this study, we developed a label-free electrochemical DNA biosensor based on ZnO NRs for detection of BCR/ABL fusion gene. Electrochemical impedance spectroscopy (EIS), cyclic voltammetry (CV), and field emission scanning electron microscope (FESEM) were utilized to characterize the fabricating process and to evaluate the biosensor performance.

2. MATERIALS AND METHODS

Platinum (Pt) thin film were deposited on silicon (Si) (100) substrates by radio frequency magnetron sputtering at incident power of 100W for 1 h using a Pt metal target (purity, 99.99%) at ambient temperature. Then, spin coating technique was used to deposit ZnO seed layer on Pt/Si surface. Ten drops of ZnO precursor were dropped on the surface of rotated film. Rotation per minute was fixed at 3000 within 1 min. After that, the film was dried at 100°C for 5 minutes to eliminate any volatile components. Well-aligned ZnO NRs were synthesized on Pt/Si substrates by chemical bath deposition method. Hexamethylenetetramine ($C_6H_{12}N_4$) and Zinc nitrate hexahydrate ($Zn(NO_3)_2{\cdot}6H2O$) were separately dissolved into deionized water in the same molar concentration at 25 °C. Then, 10 mM uniformly stirred solution was transferred into cell. Growth temperature and time were maintained at 110 °C and 1 h during the growth procedure, respectively.

Immobilization of ssDNA on ZnO/Pt/Si electrode was done by dropping 10 μL of 1 μM probe ssDNA (in 50.0 mM phosphate buffer (PBS, pH=7.0)) directly onto the film and maintained at room temperature for 1 h using electrostatic adsorption of negatively charged ssDNA molecules. Then the immobilized electrode was washed by DI water consecutively to remove unabsorbed ssDNA probe on the electrode surface. After that, 10 μL of hybridization solution (PBS, pH 7.0) containing

complementary DNA (target DNA), namely an 18-base fragment of BCR/ABL fusion gene sequence was pipetted onto the modified electrode and dried at room temperature. Then the modified electrode was rinsed with 0.1% sodium dodecylsulfate solution to remove unhybridized DNA. Cyclic voltammetry were carried out in potential ranges of 0.8 V to -0.6 V and the scanning rate of 20 mV s^{-1}. EIS measurement was done in a 0.1 M KCl solution including 1.0 mM $[Fe(CN)_6]^{3-/4-}$ with the frequency range from 10^4 to 0.1 Hz. The morphology of samples were characterized by a FESEM (FEI Sirion 200).

3. RESULTS AND DISCUSSION

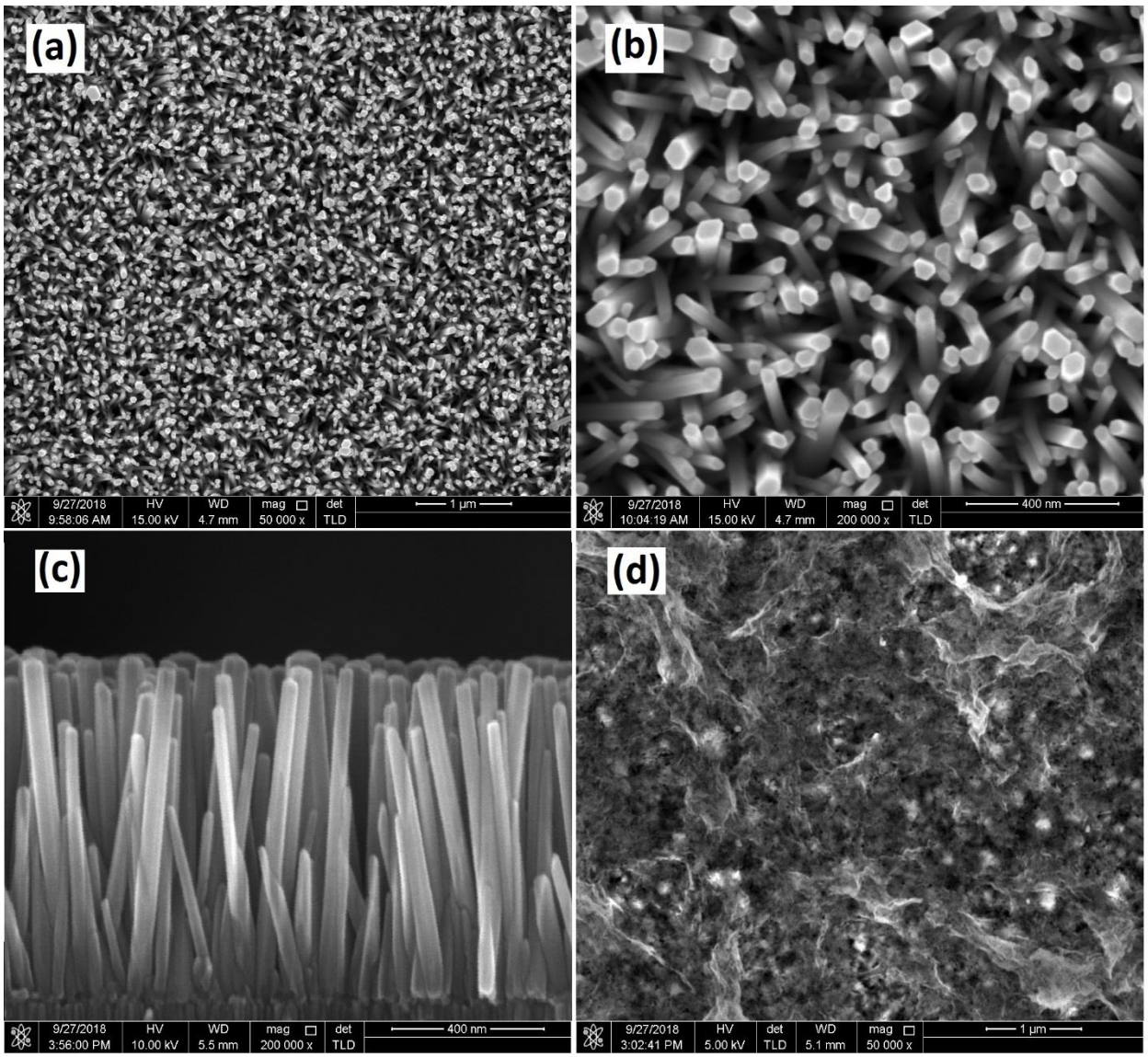

Figure 1. (a) and (b) top view FESEM images, (c) Cross-section image of ZnO NRs grown onto Pt/Si electrode (d) FESEM image of the ssDNA probe immobilized on the ZnO/Pt/Si electrode.

Figure 1a and 1b indicate a top view FESEM image of the grown ZnO NRs onto Pt/Si electrode at different magnifications. As shown in the figures, the overall grown ZnO NRs are vertically aligned

and highly dense with hexagonal faces. Furthermore, the diameter of the ZnO NRs were assessed to be in about 50 nm with uniform spatial distribution and density. Figure 1c shows the FESEM cross-section image of ZnO NRs grown on the substrate. It can be obviously observed that the well-defined ZnO NRs was successfully grown vertically on the substrate, and the average height of the ZnO NRs is 1µm. Moreover, the FESEM image of the ssDNA probe immobilized on the ZnO/Pt/Si electrode is shown in Figure 1d. The ssDNA probe immobilization onto the ZnO NRs modified electrode eventuated in a homogenous coverage which can be introduced the ZnO NR structures as a good substrate for the ssDNA immobilization.

CV analysis can provide suitable information on the surface barrier changes in the electrodes during the manufacturing process. Figure 2 reveals the CV results obtained from Pt coated on Si substrate (Pt/Si), ZnO NRs based electrode (ZnO/Pt/Si), and ssDNA probe modified nanostructured electrode (ssDNA/ZnO/Pt/Si). The cyclic voltammograms show the existence of redox peaks in all the electrodes.

As shown in figure 2, the ZnO NRs growth onto the surface of Pt/Si electrode reduces the value of the peak anodic current from 0.25 mA to 0.18 mA. It can be attributed to the insulating nature of the ZnO nanostructures which prevents the electron flow among the electrolyte and the electrode [16, 17]. A further reduction in oxidation current was detected after immobilizing ssDNA onto the nanostructure modified electrode using electrostatic interactions. It may be ascribed to the electrostatic repulsion of the negatively charged $[Fe(CN)6]^{3-/4-}$ anion and DNA phosphate backbone in the buffer solution which leads to a decrease in electron transfer kinetics [18, 19].

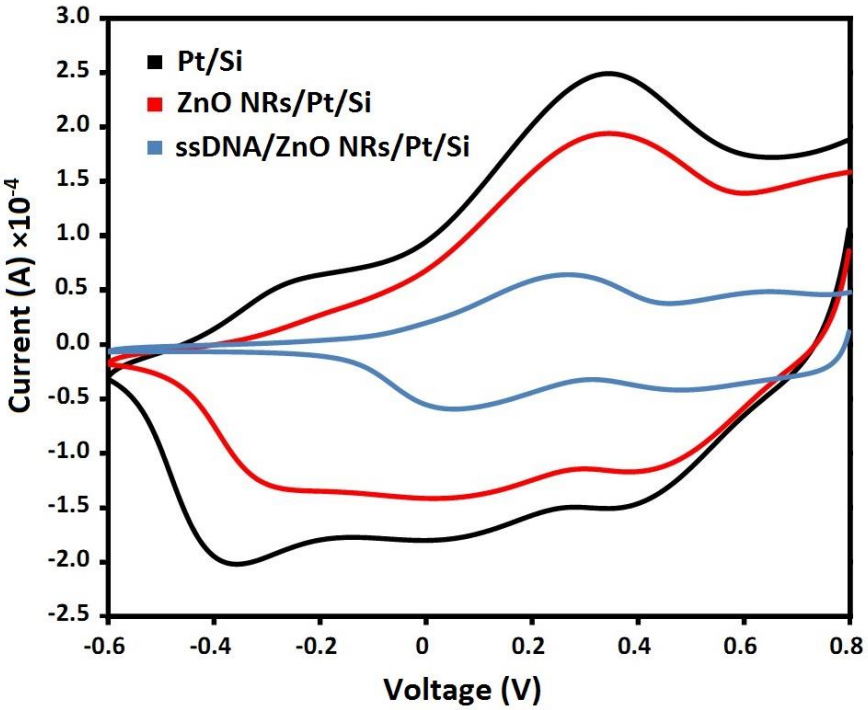

Figure 2. Cyclic voltammograms of Pt/Si, ZnO/Pt/Si, and ssDNA/ZnO/Pt/Si electrodes were recorded in 50 mM PBS solution at pH 7.0 containing 5 mM $[Fe(CN)_6]^{3-/4-}$ ions

EIS characterization was utilized to evaluate the resistance of charge transfer (R_{CT}) at the various electrodes. The R_{CT} inducing by the ions diffusion from the electrolyte to the interface of working electrode can prove the variable phase of the assembly of DNA biosensor. The various R_{CT} identified by EIS can be utilized to confirm the construction of DNA probe immobilization and the DNA hybridization process on the electrode surface [17, 20]. The Nyquist plots of EIS were recorded in 50 mM PBS solution at pH 7.0 containing 5 mM $[Fe(CN)_6]^{3-/4-}$ ions as the redox species indicated the familiar semicircle behavior. The semicircle diameter indicated the R_{CT}, which reflected the kinetics of electron transfer from the redox probes at the electrode-PBS solution interface. The Nyquist plot of ZnO/Pt/Si electrode in figure 3 shows a small value of R_{CT} compared to ssDNA/ ZnO/Pt/Si, indicating that the ZnO NRs matrix has a great electron transfer capability and a wide surface area to release $[Fe(CN)6]^{3-/4-}$ ions towards the electrode surface. The very low R_{CT} value of the Pt/Si electrode compared to the ZnO/Pt/Si electrode may be due to the nature of the conductivity of Pt [21]. Furthermore, the increase in the R_{CT} value of ssDNA/ ZnO/Pt/Si modified electrode can be related to the electrostatic repulsion of the negatively charged $[Fe(CN)6]^{3-/4-}$ anion and backbone of probe ssDNA, which confirmed the effective immobilization of ssDNA modified electrode. On the other hand, the experimental results shown that the R_{CT} in the whole phases gradually increased which can be attributed to the fact that DNA on the electrode surface being non-conductive material went against $[Fe(CN)6]^{3-/4-}$ to spread to the surface of electrode. The variations of EIS confirmed that the different steps of the preparation of suggested sensor were successful [22, 23]. The results of EIS measurements upon DNA immobilization on ZnO/Pt/Si electrode were completely consistent with that of CV technique.

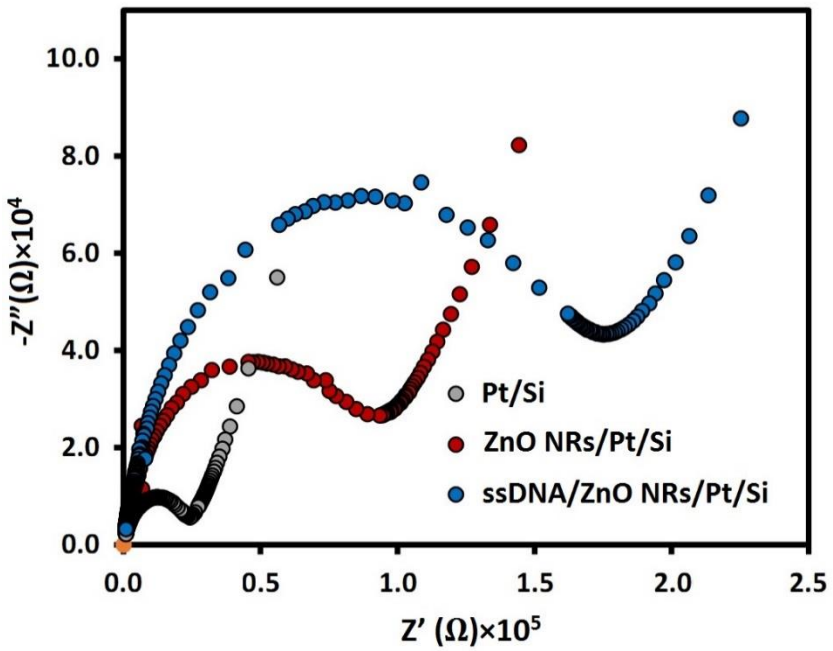

Figure 3. EIS analysis of Pt/Si, ZnO/Pt/Si, and ssDNA/ZnO/Pt/Si electrodes were recorded in 50 mM PBS solution at pH 7.0 containing 5 mM $[Fe(CN)_6]^{3-/4-}$ ions.

Figure 4a compares the impedimetric behavior of the modified biosensor that were gained when the concentration of the BCR/ABL fusion gene target DNA sequence was changed from 1.0 pM/L to 1.0

nM/L in the hybridization solution. The results indicate that the hybridization process leads to a gradual decrease of the impedimetric response. We found that the gradual reduction in the value of R_{CT} is consistent with the increase in target DNA concentration. As shown in Figure 4b, the difference of the R_{CT} value (ΔR_{CT}) before and after hybridization is linearly proportionate to the logarithm of the complementary DNA target concentrations in the range of 1.0 pM/L to 1.0 nM/L. The extracted regression equation was ΔR_{CT} (Ω) = 49106 log C (mol/L) + 616954 with the regression coefficient (R) 0.994. The detection limit was estimated to be 2.75×10^{-13} mol/L with 3σ, where σ is a relative standard deviation of the blank solution with 11 parallel measurements. These findings indicate that the modified DNA biosensor is sensitive enough for the BCR/ABL fusion gene sequence detection.

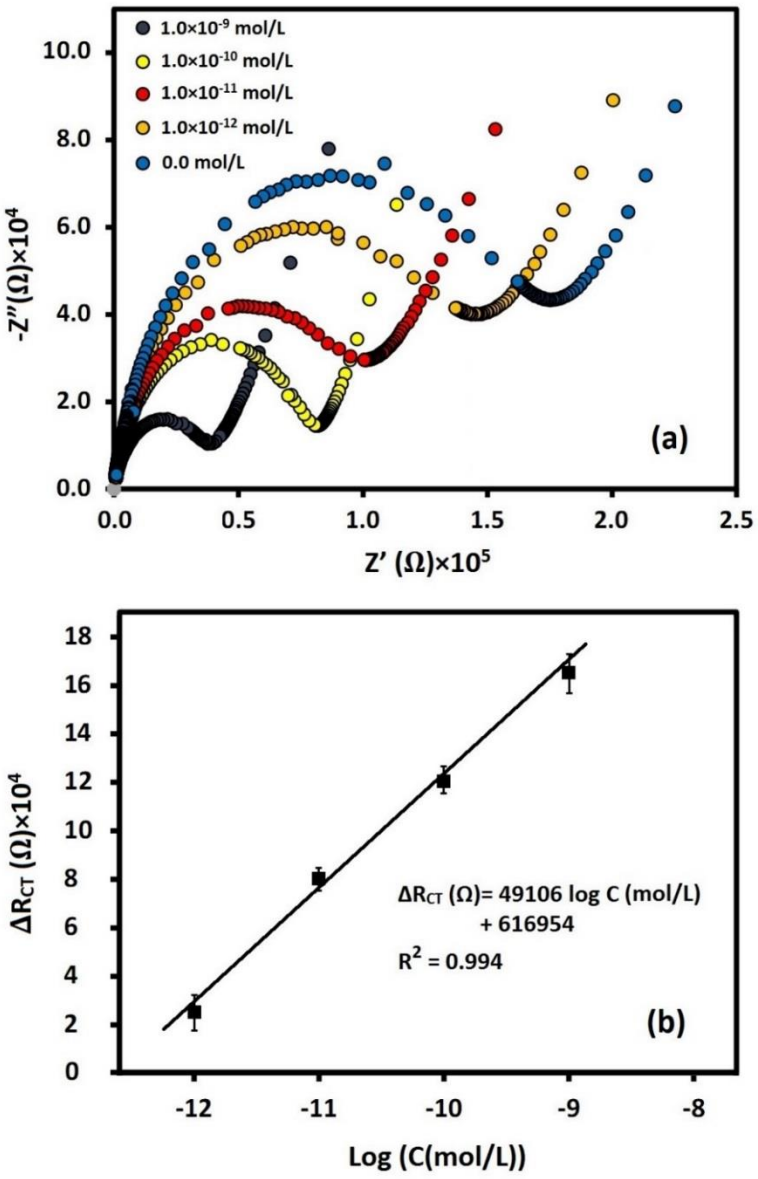

Figure 4. (a) Nyquist plots of the ssDNA/ZnO/Pt/Si biosensor before and after hybridization with different concentrations of BCR/ABL fusion gene DNA target sequences (b) The plot of ΔR_{CT} versus the logarithm of the complementary DNA concentrations.

The performance of the proposed DNA biosensor was compared with that of some other biosensors for BCR/ABL fusion gene sequence as listed in Table 1. It can be clearly seen that this suggested DNA biosensor shows a wide detection range and an excellent detection limit for testing the target DNA.

Table 1. Comparison of the proposed biosensor performance with some other DNA biosensors for BCR/ABL fusion gene sequence

References	Sensor platform	Detection methods	Detection limit (mol/L)	Detection range (mol/L)
This work	ZnO/Pt/Si probe	CV and EIS (PBS)	2.75×10^{-13}	1.0×10^{-12} to 1.0×10^{-9}
[24]	Glassy carbon surface / DNA probe	CV, EIS and DPV	3.0×10^{-12}	1.0×10^{-11} to 5.0×10^{-7}
[25]	Glassy carbon surface /graphene sheets / chitosan / PANI / AuNps / DNA probe	CV, EIS and DPV	2.11×10^{-12}	1.0×10^{-11} to 1.0×10^{-9}
[26]	Glassy carbon surface / DNA probe with terminal amino group	DPV	5.9×10^{-8}	1.25×10^{-7} to 6.75×10^{-7}
[27]	Gold surface / DNA probe (thiolated hairpin locked nucleic acids)	CV, EIS and DPV	1.2×10^{-10}	-
[28]	ITO coated glass substrate / nanostructured composite of chitosan and cadmium-telluride quantum dots / DNA probe with terminal amino group	CV and DPV	2.56×10^{-12}	1.0×10^{-6} to 1.0×10^{-11}

4. CONCLUSION

A novel DNA biosensor based on ZnO NRs/Pt for selectivity electrochemical detection of the BCR/ABL fusion gene was developed. The FESEM image revealed that ZnO NRs were synthesized on the surface of the Pt/Si substrate with a good orientation and an average diameter of 50 nm. ZnO NRs

and Pt were successfully deposited onto the surface of the electrode to significantly improve the electrochemical effective surface area and conductivity. The electrochemical changes of the ZnO layer concluded from DNA immobilization and hybridization were investigated by EIS and CV. The fabricated DNA biosensor was evaluated in the complementary target ssDNA of BCR/ABL fusion gene probe in the dynamic range from 1.0×10^{-9} to 1.0×10^{-12} mol/L which indicates a good linearity, high sensitivity and low detection limit of 2.75×10^{-13} mol/L. The results indicate that the modified DNA biosensor is sensitive enough to detect the BCR/ABL fusion gene sequence.

ACKNOWLEDGEMENT
The authors would like to thank the National Natural Science Foundation of China (no. 11405013) and the Hunan Natural Science Research Fund (no. 2018JJ2422) for the financial supports.

References

1. K. Eswar, J. Rouhi, H. Husairi, M. Rusop and S. Abdullah, *Adv. Mater. Sci. Eng*., 2014 (2014) 1.
2. R. Dalvand, S. Mahmud, J. Rouhi and C.R. Ooi, *Mater. Lett*., 146 (2015) 65.
3. J. Su, D. Wang, L. Nörbel, J. Shen, Z. Zhao, Y. Dou, T. Peng, J. Shi, S. Mathur and C. Fan, *Anal. Chem.*, 89 (2017) 2531.
4. P.A. Rasheed and N. Sandhyarani, *Biosens. Bioelectron,* 97 (2017) 226.
5. T. Adam and U. Hashim, *Biosens. Bioelectron*., 67 (2015) 656.
6. M. Cui, Y. Wang, H. Wang, Y. Wu and X. Luo, *Sens. Actuators B Chem*., 244 (2017) 742.
7. P. Mehrotra, *J. Oral Biol. Craniofac. Res*., 6 (2016) 153.
8. M. Mazloum-Ardakani, L. Hosseinzadeh and M.M. Heidari, *Microchim. Acta,* 183 (2016) 219.
9. H.L. Lund, C.B. Hughesman, K. McNeil, S. Clemens, K. Hocken, R. Pettersson, A. Karsan, L.J. Foster and C. Haynes, *Anal. Bioanal. Chem*, 408 (2016) 1079.
10. M. Manda-Mapalo, P. Khalili, D. Quintana, I. Rabinowitz and Q. Zhang, *Cancer Genet.*, 209 (2016) 481.
11. F. Li, Y. Feng, P. Dong, L. Yang and B. Tang, *Biosens. Bioelectron,* 26 (2011) 1947.
12. J. Chen, J. Zhang, L. Huang, X. Lin and G. Chen, *Biosens. Bioelectron*. 24 (2008) 349.
13. V.C. Diculescu, A.-M. Chiorcea-Paquim and A.M. Oliveira-Brett, *Trac-Trends Analyt Chem*., 79 (2016) 23.
14. E. Alipour, H. Shahabi and T. Mahmoudi-Badiki, *J. Solid State Electr.,* 20 (2016) 1645.
15. L. Lin, J. Chen, Q. Lin, W. Chen, J. Chen, H. Yao, A. Liu, X. Lin and Y. Chen, *Talanta*, 80 (2010) 2113.
16. M. Tak, V. Gupta and M. Tomar, *Biosens. Bioelectron.*, 59 (2014) 200.
17. Z. Zheng, J. Jiang, M. Zheng, C. Zhao, K. Peng, X. Lin and S. Weng, *Int. J. Electrochem. Sci*., 11 (2016) 8354.
18. A.A. Ansari, R. Singh, G. Sumana and B. Malhotra, *Analyst,* 134 (2009) 997.
19. M. Raveendran, A.F. Andrade and J. Gonzalez-Rodriguez, *Int. J. Electrochem. Sci*., 11 (2016) 763.
20. X. Cai, S. Weng, R. Guo, L. Lin, W. Chen, Z. Zheng, Z. Huang and X. Lin, *Biosen. Bioelectron.,* 81 (2016) 173.
21. S. Xu, Y. Zhang, K. Dong, J. Wen, C. Zheng and S. Zhao, *Int. J. Electrochem. Sci,* 12 (2017) 3443.
22. X. Xu, X. Weng, A. Liu, Q. Lin, C. Wang, W. Chen and X. Lin, *Anal. Bioanal. Chem.*, 405 (2013) 3097.
23. S. Xu, H. Duo, C. Zheng, S. Zhao, S. Song and G. Simon, *Int. J. Electrochem. Sci,* 14 (2019) 1248.
24. G.-X. Zhong, J.-X. Ye, F.-Q. Bai, F.-H. Fu, W. Chen, A.-L. Liu, X.-H. Lin and Y.-Z. Chen, *Sens. Actuators B Chem*., 204 (2014) 326.

25. L. Wang, E. Hua, M. Liang, C. Ma, Z. Liu, S. Sheng, M. Liu, G. Xie and W. Feng, *Biosens. Bioelectron*, 51 (2014) 201.
26. X.-H. Lin, P. Wu, W. Chen, Y.-F. Zhang and X.-H. Xia, *Talanta,* 72 (2007) 468.
27. L. Lin, X. Lin, J. Chen, W. Chen, M. He and Y. Chen, *Electrochem. Commun.*, 11 (2009) 1650.
28. A. Sharma, C.M. Pandey, G. Sumana, U. Soni, S. Sapra, A. Srivastava, T. Chatterjee and B.D. Malhotra, *Biosens. Bioelectron.*, 38 (2012) 107.